

## Use of Morphological Method to Investigate the Influence of Surface Texture on Dimensional Measurement of Additively Manufactured Parts

S. Lou<sup>1</sup>, S. B. Brown<sup>2</sup>, W. Sun<sup>2</sup>, W. Zeng<sup>1</sup>, H. S. Abdul-Rahman<sup>1</sup>, X. Jiang<sup>1</sup>, P. J. Scott<sup>1</sup>

<sup>1</sup> EPSRC Future Metrology Hub, University of Huddersfield, Queensgate, Huddersfield, HD1 3DH

<sup>2</sup> National Physical Laboratory, Engineering, Materials & Electrical Science, Hampton Road, Teddington, Middlesex, TW11 0LW, UK

[s.lou@hud.ac.uk](mailto:s.lou@hud.ac.uk)

### Abstract

The high level of surface roughness of additively manufactured (AM) parts post challenges to the applicability of different dimensional measurement techniques, including tactile, optical and XCT. Tactile measurement is traditionally considered to have the best accuracy and traceability. However, tactile measurement can be significantly affected by the mechanical filtering effect. This work sets out to investigate the influence of the mechanical filtering effect of tactile measurement on AM parts. Both experiential and simulation work are utilised to reveal this effect. Particularly the numerical simulation based on the morphological method allows the single influence factor, i.e., the tip diameter to be investigated. The maximum measurement errors caused by the stylus tip mechanical effect are determined by the convex hull points of the measurement profile, which is equivalent to using an infinitely large stylus tip. The CMM and XCT results of measuring the AM cylinder diameters are compared, along with the application of morphological method to “compensate” the mechanical filtering effect of the stylus tip.

Additive manufacturing, dimensional metrology, surface roughness, morphological method.

### 1. Introduction

Building up a component layer by layer, via additive manufacturing (AM), allows the construction of complex geometries not possible with conventional manufacturing processes. However, an insufficiency of AM is its poor surface finish with roughness ranging from a few micrometres to several hundred of micrometres. This high surface roughness of AM parts post challenges to the applicability of different dimensional measurement techniques, including tactile, optical and X-ray computed tomography (XCT).

Tactile measurement techniques, e.g., Coordinate Measurement Machines (CMMs) coupled with tactile probes, are traditionally considered to have the best accuracy and traceability. However, the measurements from a CMM can be significantly affected by the interaction of the stylus tip and the surface texture. Due to the finite size of the tip, it is unable to penetrate into all the valleys and thus the true surface is never detected. This is also known as the mechanical filtering effect [1]. Moreover, tactile measurement methods are not able to measure some of the more complex AM geometries, whose intricate forms do not permit line-of-sight. In contrast, X-ray computed tomography (XCT) can, in principle, measure both internal and external surfaces of such objects.

There are a current lack of international standards covering the dimensional verification of XCT. XCT measurement often refer back to tactile probing as the reference data, e.g., CMMs with tactile probes, because tactile CMMs can provide traceable measurement. However, when using the tactile reference for XCT, it should be noted that tactile probing does not reveal real surface, especially in case of rough surfaces, e.g. AM surfaces. Normally the rougher the surface is, the more obvious the mechanical filtering effect will be. The confidence associated with the individual measuring techniques when measuring traditionally machined parts bearing smooth

surfaces cannot be directly translated across to AM parts, where the surface roughness appears to influence the result [2, 3].

Comparisons of tactile and XCT dimensional measurement on rough surfaces are reported in recently published works [4-8]. Aloisi and Carmignato found that the deviations between CMM and XCT in measuring AM cylinder diameters are about  $Rz/2$  [4]. They further conducted a simulation study to investigate the CT surface filtering effect [5]. Schmitt and Niggemann estimated that the influence of surface texture to XCT measurement is about the mean value of  $Rz/2$  [6]. Similarly Bartscher et al. stated that the surface roughness contributes to uncertainty in the order of  $Rz/2$  as an upper limit. For their experimental case, the effect was estimated to be less than  $Rz/4$  [7]. From the experiments of Boeckmans et al, the offsets between CT and tactile measurement were in 1:1 ratio of the  $Rp$  value [8].

This paper aims to systematically investigate the influence of the mechanical filtering effect on dimensional measurement of AM processed components. Both experimental and simulation work will be utilised to reveal this effect.

### 2. Experimental analysis

#### 2.1. AM test object and its measurement

An AM test object was designed at the National Physical Laboratory (NPL) and built by Selective Laser Melting (SLM) using AlSi10Mg powders [3]. The test object incorporates both external and internal features that are accessible by traditional measuring systems, such as CMMs. The designed geometrical features have simple forms (e.g. cylinders, flats and squares) that can be characterised. See **Figure 1**. The test object is fitted onto a removable aluminium base plate. To ensure a repeatable and positive fit to the base, the base of the AM test object has been ground flat. The base plate includes three ceramic tooling spheres, which enable a unique coordinate

system to be generated. Measurement of the separation of the spheres provides a verification of scale.

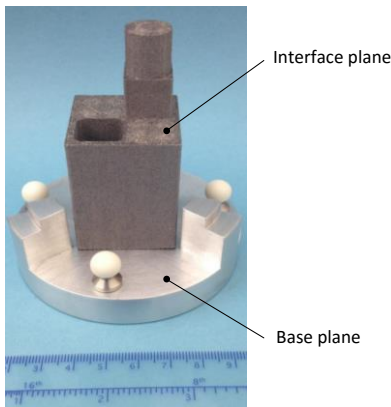


Figure 1. The NPL designed AM test object fitted onto a base plate.

Groups of measurements of the AM test object and the base plate were made on a Mitutoyo CMM Crysta Apex, with a maximum permissible error (MPEE)  $1.7+3L/1000 \mu\text{m}$ , where L is in mm [9]. Each set of measurements was repeated using tooling spheres of: 3 mm, 4 mm and 5 mm in diameter. Each set initially measured the three tooling spheres to generate a coordinate system and the top of the base plate. Measuring the top of the base plate allowed a base plane to be defined. This universal plane allows height measurements made to the AM test object on and off the base plate to be compared.

A plane was defined at the interface of the internal and external features. This interface plane was measured using 319 points. The distance between this plane and the base plane of the AM test object was calculated, allowing an examination of the offsets of the plane caused by the effect of surface roughness. The circularity of the cylinder was measured at: 23.5 mm, 26 mm, 28.5 mm and 31 mm for the internal cylinder, and for the external cylinder at: 68 mm, 70.5 mm, 73 mm and 75.5 mm from the base plate datum.

## 2.2. Measurement results

The height of the interface plane is defined as the distance between two points; the point defined as the intersection of the internal cylinder's axis with the interface plane and the point defined by the intersection of the axis of the same cylinder and the base plane. The interface plane heights are listed in Table 1 and plotted in Figure 2. It can be seen that the separation distances increase with increasing probe diameters. This conforms to the theoretical analysis that the larger the tip diameter, the closer the measured profile becomes to the macroscopic profile. The distance offsets between the No.1 and No.2, the No.2 and No.3 are  $14 \mu\text{m}$  and  $11 \mu\text{m}$  respectively.

Table 1. Interface plane heights in respect to three different stylus tip diameters (Unit: mm).

No.	Probe dia	Interface	Base	Distance
1	3	38.800	-9.992	48.792
2	4	38.799	-10.007	48.806
3	5	38.826	-9.991	48.817

The measurement results of the external and internal cylinder diameters are listed in Table 2 and Table 3 and plotted in Figure 3 and Figure 4. It is observed that all four external cylinder diameters increase with increasing tip diameter, while the four internal diameters decrease as the tip diameter increases.

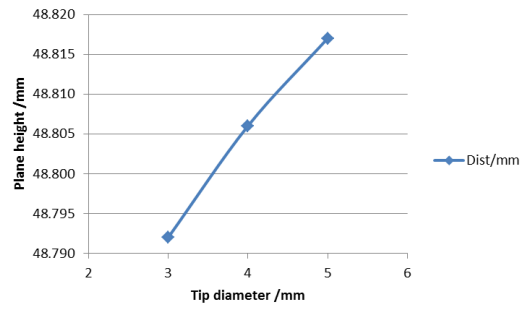


Figure 2. Variation of the offsets of the interface plane in response to stylus tip diameters.

Table 2. External cylinder diameters in respect to different stylus tip diameters (Unit: mm).

Probe dia	58.0	60.5	63.0	65.5
3	14.052	14.040	14.060	14.056
4	14.073	14.058	14.078	14.075
5	14.082	14.066	14.088	14.085

Table 3. Internal cylinder diameters in respect to different stylus tip diameters (Unit: mm).

Probe dia	13.5	16.0	18.5	21.0
3	13.721	13.716	13.727	13.755
4	13.688	13.687	13.701	13.725
5	13.676	13.672	13.682	13.716

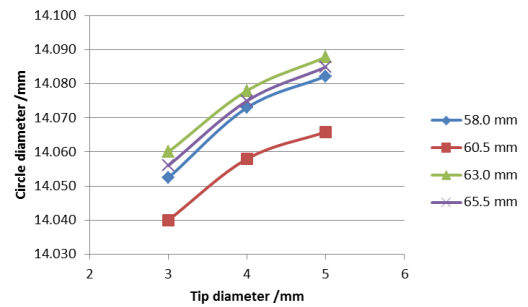


Figure 3. Variation of external cylinder diameters in response to stylus tip diameters.

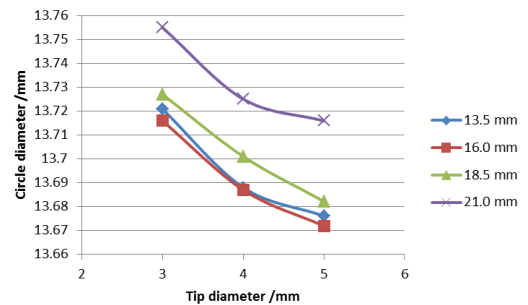


Figure 4. Variation of internal cylinder diameters in response to stylus tip diameters.

## 3. Numerical simulation by morphological method

Mathematical morphology [10] enables the numerical simulation of physical surface probing. The adopted algorithms in this work were based on morphological image processing techniques where the measured surface height map is treated as a grey-scale image; however, where the surface is curved,

these approaches are no longer valid. Recently developed computational methods based on the Alpha shape theory have removed this limitation [11, 12].

### 3.1. Simulation: varying disk probe diameters

In the simulation, the profile was measured from the interface plane of the NPL test object. The resultant relevant roughness parameters (without filtering) are Ra 38.4  $\mu\text{m}$ , Rq 51.8  $\mu\text{m}$ , Rp 211.9  $\mu\text{m}$  and Rz 339.8  $\mu\text{m}$ . The simulated probe diameters range from 0.3 mm to 12 mm. **Figure 5** presents three closing envelopes of 3 mm, 4 mm and 5 mm stylus tip diameters respectively and the corresponding Gaussian Least Square (LS) planes of these probe diameters. It can be seen, from **Figure 5**, the larger the probe diameter, the more the closing envelope approaches the local significant profile peaks and, thus, the greater the offset in height. The lines representing the Rp and Rz/2 height plane are also marked in **Figure 5** to indicate the limits of the height offset. For planar surfaces, the extreme case that the used disk probe is infinitely large will produce the largest offset, Rp. Nonetheless, the height offsets produced by the 3 mm, 4 mm and 5 mm disk probes were within this limit and much smaller than Rp, being around 6 % of Rp. The Rz/2 plane is 42  $\mu\text{m}$  below the Rp plane, which indicates that the largest valley is smaller than the largest peak in amplitude. If these two are with the same amplitude, then the Rp and Rz/2 plane should overlap.

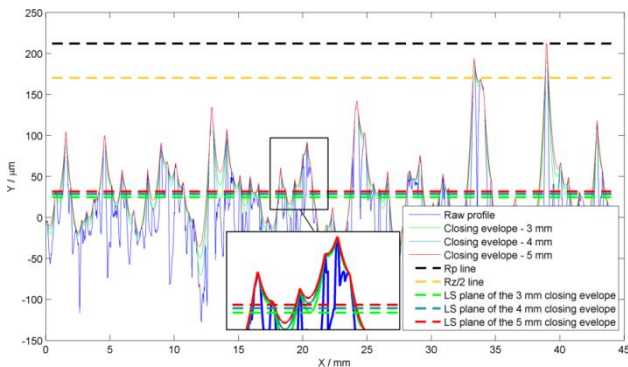


**Figure 5.** Closing envelopes of different disk radii and various limiting planes.

In the second case, the previously used AM profile was wrapped around a circle of diameter 14 mm. **Figure 6** shows the closing envelope of a 5 mm disk, which is used to represent the numerical simulation of scanning the circumference of an external cylinder (diameter: 14 mm). Please note the round profile diameter is suppressed by 13 mm to enable a better visualisation of surface texture. The LS diameter, from the closing envelope, is slightly larger than that of the original measured profile, indicating the offset effect of the probe diameter to dimension measurement. In the extreme case of using an infinitely large probe diameter, the stylus tip will only contact a limited number of points on the profile. Theoretically these contact points are the vertices of the convex hull of the round profile. The green circle in **Figure 6** indicates the LS circle produced by the convex hull points. The diameter of this green circle, instead of the diameters of the Rp and Rz/2 circles, is the limit that a probe diameter can produce. In any case, it should be smaller than the Rp circle.

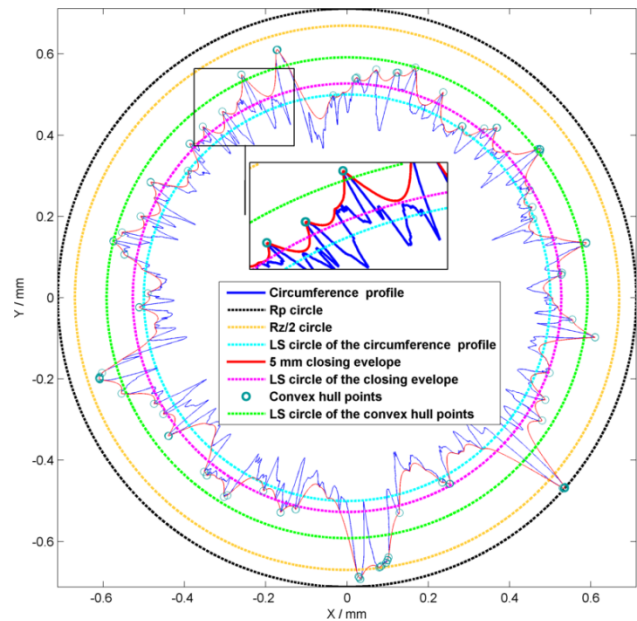


**Figure 6.** Closing envelope of the 5 mm disk and various limiting circles.

The full results of applying the whole set of probe diameters are listed in **Table 4** and plotted in **Figure 7**, where it can be seen that larger probe diameters will produce a greater offset in both plane heights and cylinder diameters. This offset, due to probe diameter, results in the diameter of the external cylinder increasing with an increase of probe diameter and the diameter of the internal cylinder decreasing with an increase in probe diameter. The offset diameter will gradually approach the limit, namely the one determined by the convex hull points.

**Table 4.** Plane height offset and external/internal cylinder diameters resulted from a set of probe diameters.

Probe dia /mm	Plane height offset / $\mu\text{m}$	Ex-cylinder dia /mm	In-cylinder dia /mm
0.3	3.1	14.001	14.000
0.5	5.5	14.001	14.000
0.7	7.9	14.002	13.999
1	11.7	14.003	13.998
1.5	16.1	14.004	13.996
2	19.7	14.006	13.993
2.5	22.4	14.007	13.990
3	24.6	14.009	13.988
4	28.6	14.011	13.984
5	31.7	14.013	13.980
6	34.1	14.014	13.978
8	38.1	14.017	13.973
10	41.8	14.019	13.969
12	45.1	14.021	13.965

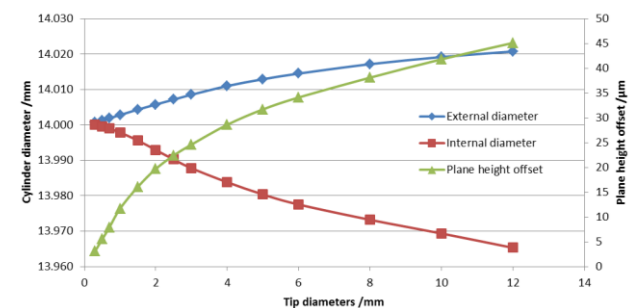


**Figure 7.** Plane height offsets and cylinder diameters variation with stylus tip diameter selection.

### 3.2. Simulation: varying surface roughness

In this simulation, the probe disk diameter is fixed to 4 mm, while the seven examined surfaces vary in their roughness ranging from 0.9  $\mu\text{m}$  to 37.5  $\mu\text{m}$ . These surfaces are measured from the casting Rubert plate which has a similar surface texture to that of AM processed surfaces. The simulated result of using the morphological method is listed in **Table 5** and plotted in **Figure 8**. It is shown that the rougher the surface is, the larger offset the probe produces for both the plane height and external/internal diameters. However, even for the roughest surface, the offset obtained from the simulation is much smaller than  $R_p$ , being only 6~16% of  $R_p$ .

**Table 5.** Closing envelope of the 5 mm disk and various limiting circles.

Ra / $\mu\text{m}$	Rp / $\mu\text{m}$	Plane offset / $\mu\text{m}$	Ex-cyl diam /mm	Dev ( $\mu\text{m}$ )	Int-cyl diam /mm	Dev / $\mu\text{m}$
0.9	3.4	0.2	14.000	0	14.000	0
2.5	11.3	1.6	14.001	1	13.999	-1
4.3	18.0	2	14.001	1	13.999	-1
7.0	40.8	2.8	14.001	1	13.999	-1
11.8	42.5	5.2	14.002	2	13.997	-3
23.1	103.7	10.9	14.003	3	13.996	-4
37.5	198.1	31.2	14.012	12	13.981	-19

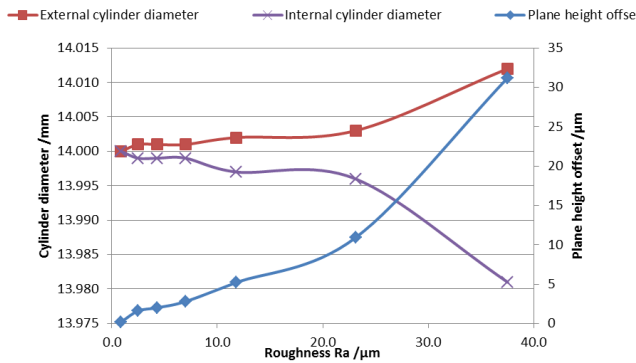


**Figure 8.** Plane height offset and cylinder diameter variation in response to surface roughness.

#### 4. Comparison and discussion

The comparison of CMM (stylus tip diameter 3 mm) and XCT on measuring cylinder diameters at eight heights is listed in **Table 6** and **Table 7**. To compensate the CMM stylus mechanical filtering effect, the morphological method is applied to the XCT generated circumference profiles. The experimental results show that the deviations between CMM and XCT are close to the  $R_p$  value 211.9  $\mu\text{m}$ . Even if it is assumed that XCT results are more accurate than CMM [3, 5], the application of the morphological method to “compensate” the CMM mechanical filtering effect can only reduce a limited number of deviations. Even using the convex hull points to enable the maximum compensation can only compensate up to a quarter of the deviations.

The morphological method implies that the  $R_p$  dimensional deviation between CMM and XCT when measuring rough surfaces, e.g. AM surfaces, is not only caused by the tactile stylus mechanical filtering effect. From the tactile measurement side, there are more factors that can influence the measurement result, e.g., the scanning speed and the probe force. The other issue is that the morphological method is applied to the profile data. Surfaces are three-dimensional and so is the probing tip. Thus the surface geometry in the neighbourhood will have an impact on the measurements. The rougher the surface is, the greater the influence the surface has

on the measurement taken by the CMM. On the XCT measurement side, the research work is designed to investigate how XCT measurement will deviate from the reference.

**Table 6.** Cylinder diameters results from CMM measurement, XCT measurement and applying the morphological method to XCT measurement, (Units: mm).

Height	CMM	XCT1 (raw)	XCT2 (3 mm rolling ball)	XCT3 (Max rolling ball)
23.5	13.671	13.978	13.961	13.926
26	13.671	13.968	13.942	13.893
28.5	13.706	13.975	13.958	13.923
31	13.733	13.972	13.956	13.914
68	14.057	13.853	13.865	13.893
70.5	14.042	13.855	13.868	13.895
73	14.061	13.858	13.868	13.898
75.5	14.058	13.848	13.870	13.884

**Table 7.** Comparison of the cylinder diameters results from CMM and XCT measurements applying the morphological method to XCT measurement, (Units: mm).

Height	CMM-XCT1	CMM-XCT2	CMM-XCT3
23.5	-0.307	-0.290	-0.255
26	-0.297	-0.271	-0.222
28.5	-0.269	-0.252	-0.217
31	-0.239	-0.223	-0.181
68	0.204	0.192	0.164
70.5	0.187	0.174	0.147
73	0.203	0.193	0.163
75.5	0.210	0.188	0.174

#### 5. Conclusion and future work

AM processes tend to produce very rough surfaces. The mechanical filtering effect of tactile measurement can be prominent when measuring AM rough surfaces. Both experimental and simulation work are utilised to reveal this effect. In particular the numerical simulation based on the morphological method allows the single influence factor, i.e. the stylus tip diameter, to be investigated. The simulation results of the varying tip diameters basically agree with the experimental work. For cylinder diameter measurement, the maximum measurement errors caused by the probe mechanical effect are determined by the convex hull points, which is equivalent to using an infinitely large probe.

The CMM and XCT results from measuring the cylinder diameters of the test object are compared. Moreover the morphological method is applied to XCT measurement data in order to “compensate” the CMM mechanical filtering effect when taking the CMM results as the references. The deviations between CMM and XCT experimental results are of the scale of  $R_p$ . Morphological compensation can reduce a small portion of this deviation, which suggests that there may be other factors contributing to these deviations.

A key area of future work is the investigation of the Gaussian-like low-passing filtering effect caused by the partial volume effect of the XCT system.

#### Acknowledgement

The authors would like to personally thank their colleagues for their assistance and due diligence throughout this work. In particular they would like to thank, from NPL: Sean Woodward, Andy Sharpe and Martin Dury. This work was supported by the UK government’s Department for Business, Energy and

Industrial Strategy. From Huddersfield University, the authors gratefully acknowledge the UK's Engineering and Physical Sciences Research Council (EPSRC) funding of the Future Advanced Metrology Hub (EP/P006930/1).

## References

- [1] Weckenmann A., Estler T., Peggs G., McMurtry D. 2004 *CIRP Ann.*, **53** (2), 657-684.
- [2] Leach R 2014 Measurement Good Practice Guide No 37: The measurement of surface texture using stylus instruments.
- [3] Brown S, Sun W, McCarthy M B, Woolliams P 2016 *Proc. ASPE Summer Topical* 200-205.
- [4] Aloisi V, Carmignato S 2016 *Case Stud. Nondestr. Test. Eval.* **6** (B), 104-110.
- [5] Carmignato S, Aloisi V, Medeossib F, Zaninia F, Savio E 2017 *CIRP Ann.* in press.
- [6] Schmitt R., Niggemann C. 2010 *Measurement Science and Technology*, **21** (5): 054008.
- [7] Bartscher M, Neukamm M, Koch M, Neuschaefer-Rube U 2010 *10th European Conference on Non-Destructive Testing*, Moscow, Russia.
- [8] Boeckmans B, Tan Y, Welkenhuyzen F, Guo Y S, Dewulf W, Kruth J – P 2015 *Proc. of 15th Euspen Int. Conf.* 189-190.
- [9] ISO 10360-2 2009 *Geometrical product specifications (GPS) -- Acceptance and reverification tests for coordinate measuring machines (CMM) -- Part 2: CMMs used for measuring linear dimensions.*
- [10] Serra J 1982 *Image Analysis and Mathematical Morphology* Academic Press, New York
- [11] Lou S, Jiang X, Scott P J 2013 *Proc. R. Soc. A*, **469**(2159): 20130150.
- [12] Lou S, Jiang X, Scott P J 2014 *Meas. Sci. Technol.* **6**(25): 065005.